Level of RUNX1 activity is critical for leukemic predisposition but not for thrombocytopenia

Iléana Antony-Debré, Vladimir T Manchev, Nathalie Balayn, Dominique Bluteau, Cécile Tomowiak, Céline Legrand, Thierry Langlois, Olivia Bawa, Lucie Tosca, Gérard Tachdjian, et al.

Regular Article

HEMATOPOIESIS AND STEM CELLS

Level of RUNX1 activity is critical for leukemic predisposition but not for thrombocytopenia

Iléana Antony-Debré,[1-4] Vladimir T. Manchev,[1,2,4] Nathalie Balayn,[1,2,5] Dominique Bluteau,[1,2,5,6] Cécile Tomowiak,[1,2,5,7] Céline Legrand,[1,2,5] Thierry Langlois,[1,2,5] Olivia Bawa,[2] Lucie Tosca,[8] Gérard Tachdjian,[8] Bruno Leheup,[9,10] Najet Debili,[1,2,5] Isabelle Plo,[1,2,5] Jason A. Mills,[11] Deborah L. French,[11] Mitchell J. Weiss,[12] Eric Solary,[1,2,5] Remi Favier,[1,13] William Vainchenker,[1,2,5] and Hana Raslova[1,2,5]

[1]Institut National de la Santé et de la Recherche Médicale, Villejuif, France; [2]Gustave Roussy, Villejuif, France; [3]Hématologie Biologique, Université Paris-Est Créteil, Hôpital Henri Mondor, Créteil, France; [4]Université Paris Diderot, Paris, France; [5]Université Paris Sud, Villejuif, France; [6]Ecole Pratique des Hautes Etudes, Paris, France; [7]Centre Hospitalier Universitaire de Poitiers, Service d'Oncologie Hématologique et Thérapie Cellulaire, Poitiers, France; [8]Institut National de la Santé et de la Recherche Médicale U935-Hôpitaux Universitaires Paris-Sud, Assistance Publique-Hôpitaux de Paris Service d'Histologie Embryologie et Cytogénétique, Clamart, France; [9]Centre Hospitalier Universitaire de Nancy, Pôle Enfant, Service de Médecine Infantile et de Génétique Clinique, Vandoeuvre-Les-Nancy, France; [10]Faculté de Médecine, Université de Lorraine, Vandoeuvre-Les-Nancy, France; [11]Department of Pathology and Laboratory Medicine, and [12]Division of Hematology, The Children's Hospital of Philadelphia, Philadelphia, PA; and [13]Assistance Publique-Hôpitaux de Paris, Hôpital Trousseau, Service d'Hématologie Biologique, Paris, France

Key Points

- A half loss of RUNX1 activity leads to defects in primitive erythropoiesis, megakaryopoiesis, and proplatelet formation.
- An almost complete loss of RUNX1 activity leads to the amplification of the granulomonocytic compartment with increased genomic instability.

To explore how *RUNX1* mutations predispose to leukemia, we generated induced pluripotent stem cells (iPSCs) from 2 pedigrees with germline *RUNX1* mutations. The first, carrying a missense *R174Q* mutation, which acts as a dominant-negative mutant, is associated with thrombocytopenia and leukemia, and the second, carrying a monoallelic gene deletion inducing a haploinsufficiency, presents only as thrombocytopenia. Hematopoietic differentiation of these iPSC clones demonstrated profound defects in erythropoiesis and megakaryopoiesis and deregulated expression of RUNX1 targets. iPSC clones from patients with the *R174Q* mutation specifically generated an increased amount of granulomonocytes, a phenotype reproduced by an 80% RUNX1 knockdown in the H9 human embryonic stem cell line, and a genomic instability. This phenotype, found only with a lower dosage of RUNX1, may account for development of leukemia in patients. Altogether, RUNX1 dosage could explain the differential phenotype according to *RUNX1* mutations, with a haploinsufficiency leading to thrombocytopenia alone in a majority of cases whereas a more complete gene deletion predisposes to leukemia. (*Blood*. 2015; 125(6):930-940)

Introduction

RUNX1 protein is the α subunit of the core-binding factor (CBF) transcriptional complex. The protein contains an N-terminal Runt homology domain that binds to DNA and to CBFβ, the β subunit of CBF, and a C-terminal transactivation domain. Germline alterations in the *RUNX1* gene are responsible for the familial platelet disorder (FPD) with a predisposition to acute myeloid leukemia (AML; OMIM 601399),[1] a rare constitutive disorder that associates a moderate thrombocytopenia with a variable propensity to develop acute leukemia. Whereas all the germline *RUNX1* alterations found in FPD/AML lead to thrombocytopenia, evolution to leukemia depends on the type of mutations (ie, mutations maintaining CBFβ-binding properties) to generate dominant-negative (DN) proteins that favor leukemic evolution, whereas mutations inducing haploinsufficiency only rarely display leukemic development.[2] *RUNX1* alterations that predispose to leukemia, mainly DN-like mutants,[3,4] deregulate critical hematopoietic stem cell (HSC) and progenitor target genes such as *NR4A3*,[4] leading to the amplification of a pool of cells susceptible to acquiring additional somatic mutations, sometimes affecting the second *RUNX1* allele.[5]

FPD/AML is a suitable model for studying the defects in megakaryopoiesis that lead to thrombocytopenia. This disease can also be used to explore the initial events in leukemogenesis, because somatic alterations in the *RUNX1* gene are involved in sporadic myeloid malignancies. Chromosomal translocations that involve the *RUNX1* gene are commonly observed in AML,[6] whereas *RUNX1* gene mutations are identified in 6% to 32% of AML.[7-9] Mutations in *RUNX1* are also detected in 8% to 15% of chronic myelomonocytic leukemias[10,11] and 9% of early-stage myelodysplastic syndromes (MDSs).[12] The fact that *RUNX1* mutations are detected at an early stage in MDSs, before acute leukemia occurrence, argues for an early event in leukemic transformation.[13]

Submitted June 30, 2014; accepted December 2, 2014. Prepublished online as *Blood* First Edition paper, December 9, 2014; DOI 10.1182/blood-2014-06-585513.

I.A.-D. and V.T.M. contributed equally to this study.

The online version of this article contains a data supplement.

The publication costs of this article were defrayed in part by page charge payment. Therefore, and solely to indicate this fact, this article is hereby marked "advertisement" in accordance with 18 USC section 1734.

Analysis of mouse models indicated that RUNX1 is a key regulator of definitive hematopoiesis, including HSC emergence.[14] In adult murine hematopoietic compartments, RUNX1 is dispensable for HSC maintenance, but it negatively regulates myeloid progenitors while promoting lymphopoiesis and megakaryopoiesis.[15,16] Regarding primitive hematopoiesis, an active yolk sac–derived erythropoiesis[14] and a normal number of primitive erythroid progenitors were observed in *Runx1* knockout (KO) mice, but primitive erythrocytes had an abnormal morphology and a reduced expression of Ter119, *Klf1*, and *Gata1*.[17] Conditional *Runx1* KO led to the development of a myeloproliferative syndrome but failed to reproduce the leukemic development observed in 35% of FPD/AML patients.[15]

Induced pluripotent stem cells (iPSCs)[18] offer a new opportunity to model inherited human diseases in vitro and allow the investigation of initial pathogenic events that may occur during embryogenesis. Here, we generated iPSCs from FPD/AML patients with 2 different pedigrees: one harbored the DN-like mutation *R174Q*,[4] and the other harbored a monoallelic *RUNX1* deletion producing a true haploinsufficiency.[2] We first observed that RUNX1 played a crucial role in regulating the first wave of human primitive hematopoiesis, giving rise to erythroid and megakaryocytic (MK) cells. We noticed also that the phenotype induced by the R174Q mutant was similar to almost complete *RUNX1* knockdown in human embryonic stem cells (hESCs), indicating that the *R174Q RUNX1* mutation should affect the binding of the remaining wild-type (WT) RUNX1 protein to CBFβ to induce an almost complete loss of function.[3] Most importantly, we noticed that increased genomic instability of the granulomonocytic cell population depended on the dosage of functional RUNX1, which was associated with decreased expression of *GADD45A*[19] as well as other p53 targets. Overall, these results show that the residual activity of WT RUNX1 protein would impact the risk for development of leukemia in FPD/AML patients.

Material and methods

Cell culture

Human dermal fibroblasts (HDFs) were derived from skin biopsies of patients after informed consent in accordance with the Declaration of Helsinki. The study was approved by the Ethics Committee of INSERM RBM 01-14 for the project "Network on the inherited diseases of platelet function and platelet production."

HDFs were cultured in F10 Glutamax medium (Invitrogen, Cergy-Pontoise, France) with 20% fetal bovine serum (Invitrogen, Cergy-Pontoise, France). H9 hESC lines (National Institutes of Health code WA09) were obtained from WiCell Research Institute. iPSCs and hESCs were maintained in an undifferentiated state on irradiated mouse embryonic fibroblasts in hESC medium, as previously described.[20] The use of hESCs was approved by Agence de la Biomédecine, No. R04-0020 and No. C04-0019. OP9 cells (Riken Institute, Wako, Japan) were maintained on gelatinized dishes.

iPSC generation

HDF transduction with the STEMCCA lentivirus was performed at passage 4 or 5. HDFs were transduced twice at 12-hour intervals. HDFs (5×10^4) were then plated on mouse embryonic fibroblasts and gelatin; 24 hours later, the medium was replaced by hESC medium and was changed every day. The ESC-like colonies were picked up separately between day 30 and day 45 and cultivated as for hESC culture.[21] One iPSC control cell line (C1/CHOPWT2.2) has already been described.[22]

Hematopoietic differentiation on OP9 cells

To differentiate iPSCs in hematopoietic cells, previously described protocols using coculture on OP9 and cytokines; vascular endothelial growth factor 20 ng/mL (Miltenyi Biotech) added at day 0; and stem cell factor 25 ng/mL (Biovitrum AB, Stockholm, Sweden), interleukin-3 10 ng/mL (Miltenyi Biotech), erythropoietin 2 U/mL (Amgen, Thousand Oaks, CA), and thrombopoietin 20 ng/mL (Kirin Pharma Company, Tokyo, Japan) added at day 7 of culture were used.[20]

Clonogenic progenitor assays

HSC progenitors were sorted on the expression of CD34 and CD43 at day 11 or day 14 and were plated in triplicate at a density of 1.5×10^3 cells per milliliter in human methylcellulose medium H4434 (StemCell Technologies, Vancouver, BC, Canada) to quantify erythroid and colony-forming unit–granulocyte macrophage (CFU-GM) progenitors at a density of 3×10^3 cells per milliliter in serum-free fibrin clots to quantify MK progenitors. MK progenitors were stained with an anti-CD41a monoclonal antibody (BD Biosciences, Le Pont de Claix, France), as previously described.[20] Images were obtained with AxioVision 4.6 software. The same software was used to measure the CFU-GM colony size.

Gene expression analysis by conventional and quantitative real-time PCR

Genomic DNAs and RNAs were extracted by using QIAmp DNA Mini Kit or RNeasy Micro Kit (QIAGEN, Courtaboeuf, France). Reverse transcription of RNA was performed with SuperScript Vilo cDNA Synthesis Kit (Invitrogen, Cergy Pontoise, France). Quantitative real-time polymerase chain reactions (qRT-PCRs) and qPCRs were performed on a 7500 Real-Time PCR system using SYBR-Green PCR Master Mix (Applied Biosystems, Saint-Aubin, France). Expression levels of genes were normalized to housekeeping genes *PPIA* and *L32*. Primers are listed in supplemental Table 1 (available online on the *Blood* Web site).

Statistical analyses

Data are presented as means (± standard deviation) or with 95% confidence intervals of the mean. Statistical significance was determined by Student *t* test. $P < .05$ was considered statistically significant. For transcriptome analysis, an analysis of variance test was performed with a *P* value threshold of $P < .001$. Other methods are provided in supplemental Data.

Results

RUNX1 alterations induce a defect in erythroid and MK cell output

To compare the consequences of two germline *RUNX1* alterations, one leading to an increase in leukemia predisposition (*R174Q* mutation, pedigree A) and the other to thrombocytopenia alone (monoallelic deletion, pedigree D), four iPSC lines were derived from FPD/AML patient skin fibroblasts. The 2 pedigrees have been described previously.[2,4] The strategy of deriving iPSCs and their characterization is shown in supplemental Figures 1-3. We selected 1 iPSC clone derived from each of 2 distinct members of pedigree A (AII_1, AII_2) and 2 iPSC clones derived from pedigree D (D(a) and D(b)). Three independent control iPSC lines (C1, C2, and C3) were used as references for all experiments. All iPSC lines were passaged 15 to 20 times to remove memory of origin, which may interfere with differentiation to downstream lineages.[23,24] Deep sequencing analysis identified 109 de novo mutations for AII_1, 82 for AII_2, and 9 for D(a). The mutations of genes that could play a role in hematopoiesis were confirmed by Sanger sequencing (supplemental Table 2). However, the results showing that the same gene was never mutated in more than 1 patient sample suggest that the common phenotype observed in all FPD/AML patients studied here is exclusively linked to the germline *RUNX1* alteration and not to the randomly acquired mutations. The

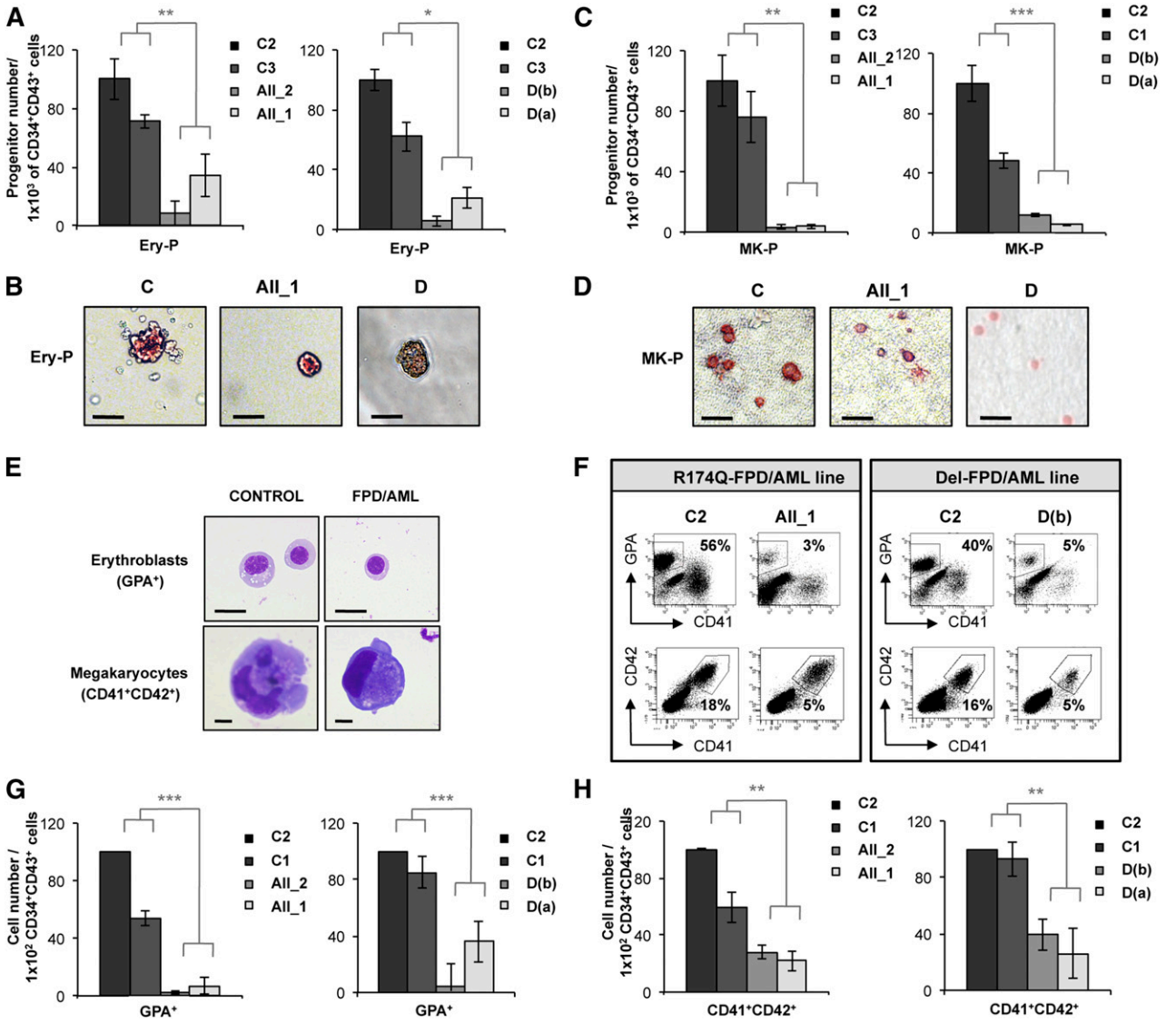

Figure 1. Deep decrease in erythroid and MK potential of progenitors derived from FPD/AML iPSC lines. All_1 and All_2 are iPSC clones of 2 patients from pedigree A; D(a) and D(b) are 2 clones of 1 patient from pedigree D; and C1, C2, and C3 are control iPSC lines. Cell numbers were normalized in all experiments to those produced by the C2 clone, which was reported in each experiment as a fixed value of 100. (A-D) $CD34^+CD43^+$ cells sorted at day 11 and tested for their colony-forming potential. (A-B) Methylcellulose assay. (A) The histograms present the numbers of erythroid progenitors (Ery-P) in 1 representative experiment of 3, each in triplicate. (B) Pictures of primitive erythroid colonies (Ery-P). (C-D) Fibrin clot culture. (C) The histograms present the numbers of MK progenitors (MK-P) in 1 representative experiment of 4, each in triplicate. (D) Pictures of primitive MK colonies (MK-P) after CD41 immunostaining. (A,C) Error bars represent ± standard deviation (SD) of triplicate. (B,D) Scale bar = 50 μm. (E-H) Analysis of hematopoietic populations at day 18 from progenitors sorted at day 11. (E) May-Grünwald-Giemsa staining of erythroblasts (GPA^+) and MKs ($CD41^+CD42^+$) derived from iPSC lines. Scale bar = 10 μm. (F) Fluorescence-activated cell sorter (FACS) analysis of erythroid cells and MKs from FPD/AML iPSC lines in 1 representative experiment. (G) Absolute number of generated erythroid cells normalized to 1×10^2 plated progenitors. The histograms show average of the cell number obtained in 5 independent experiments for pedigree A and 3 for pedigree D. (H) Absolute number of generated MKs normalized to 1×10^2 plated progenitors. The histograms show average of the cell number obtained in 3 independent experiments for both pedigrees. (G-H) Error bars represent ± SD of the average. $^*P < .05$; $^{**}P < .01$; $^{***}P < .001$; Student *t* test.

protocols of hematopoietic differentiation are described in supplemental Figure 4. Hence, we studied the impact of *RUNX1* alterations on progenitors generated by culturing $CD34^+CD43^+$ cells obtained on day 11, focusing on erythroid and MK cells, and those occurring at day 14, focusing on granulomonocytic cells. When assessing the colony-forming potential of $CD34^+CD43^+$ cells sorted at day 11, we observed a decrease in the number of erythroid progenitors generated from the *RUNX1 R174Q* mutated as well as *RUNX1* haploinsufficient iPSC clones (Figure 1A-B). We also detected a threefold decrease in MK progenitor number for both pedigrees (Figure 1C-D). $CD34^+CD43^+$ cells sorted at day 11 were also cultured on OP9 stromal cells in liquid medium (supplemental Figure 4A), demonstrating a decrease in the percentage of erythroid (GPA^+) and MK ($CD41^+CD42^+$) populations at day 18 in cells derived from the 2 pedigrees (Figure 1E-F). The absolute numbers of erythroid (GPA^+) and MK cells generated from 1×10^2 $CD34^+CD43^+$ progenitors were decreased for both the *RUNX1 R174Q* mutation and *RUNX1* deletion iPSC clones (Figure 1G-H). Strikingly, these results demonstrate that, in humans, RUNX1 plays an important role in the first wave of hematopoiesis yielding primitive erythroid and MK cells.

MKs derived from FPD/AML iPSCs display a profound defect in proplatelet formation

When $CD41^+CD42^+$ MKs were sorted after 14 days of coculture and analyzed 5 days later (Figure 2A), the percentage of proplatelet-forming

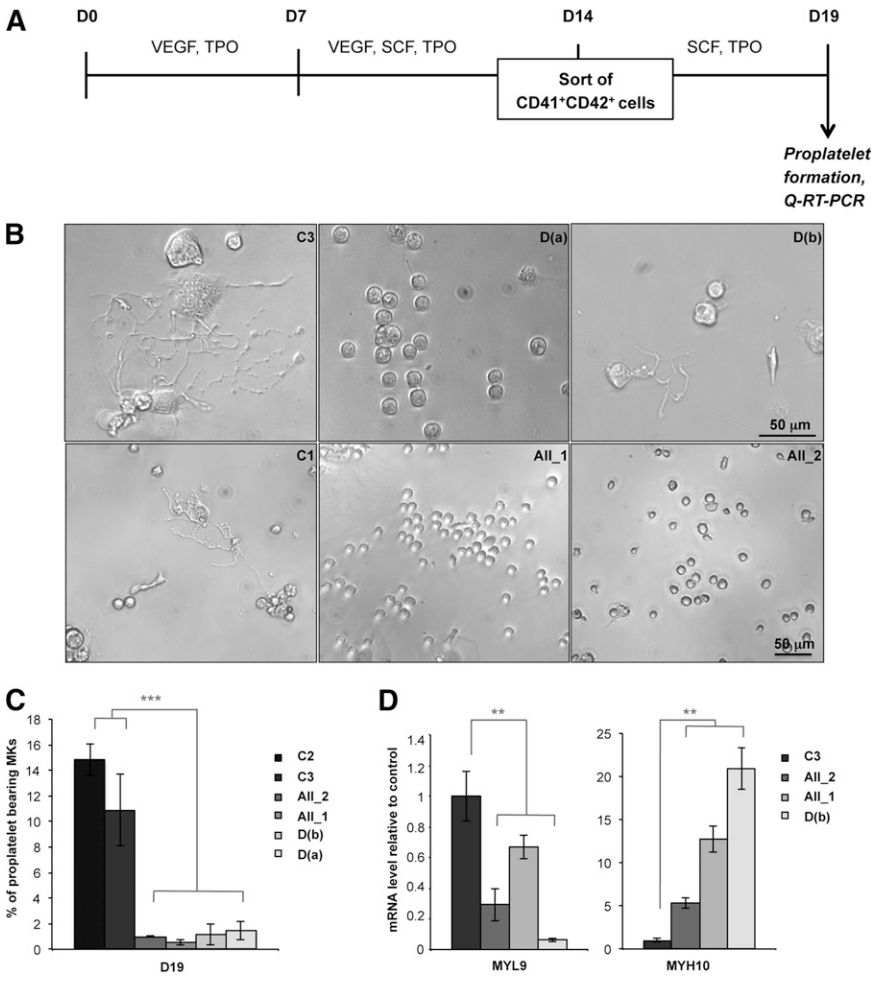

Figure 2. Defect in proplatelet formation by MK cells derived from FPD/AML iPSC lines. (A) Schema of protocol used for MK differentiation. iPSC lines were seeded on OP9 cells with vascular endothelial growth factor (VEGF) and thrombopoietin (TPO) at day 0. After 7 days, stem cell factor (SCF) was added to the culture medium. MK ($CD41^+CD42^+$) cells were sorted at day 14 and further cultured in the presence of TPO and SCF. Analysis of proplatelet formation and qRT-PCR were performed at day 19. (B) Representative microscopic images representing control and patient proplatelet-forming MKs. (C) The percentage of proplatelet-forming MKs was estimated by counting MKs exhibiting 1 or more cytoplasmic processes with areas of constriction. A total of 200 cells per well was counted. The histograms show 1 representative experiment of 5, each in triplicate. Error bars represent ± SD of triplicate. (D) qRT-PCR analysis of *MYL9* and *MYH10* expression level in MKs. The histograms show 1 representative experiment of 4 for *MYL9* and 5 for *MYH10*, each in triplicate. Data are normalized to *PPIA* and *L32* transcript level, and expression is compared with control C3. Similar results were obtained but only results normalized to *PPIA* are shown. Error bars represent ± SD of triplicate. $^{**}P < .01$; $^{***}P < .001$; Student *t* test.

MKs was decreased at least 10-fold in patient iPSCs compared with control iPSC-derived MKs (Figure 2B-C). Since RUNX1 is a positive or negative regulator of cytoskeleton components involved in proplatelet formation (MYL9, MYH9)[25] or in ploidization (MYH10),[26] we examined the expression of these genes. As observed in MKs derived from patient progenitors,[25] MYL9 expression level was decreased whereas MYH10 expression was increased in MKs obtained from patient iPSCs, whatever the *RUNX1* alteration (Figure 2D), demonstrating that the defect in megakaryopoiesis is independent of the type of *RUNX1* alteration.

RUNX1 R174Q mutation specifically affects the output of granulomonocytes

When we assessed the GM colony-forming potential of $CD34^+CD43^+$ cells sorted at day 14 (supplemental Figure 4A), we observed a significant twofold increase in the number of CFU-GM colonies in the 2 patients with *R174Q* mutation compared with the 3 controls (Figure 3A), but not in the patient with a monoallelic *RUNX1* deletion (Figure 3B). The size of GM colonies generated from *R174Q* iPSCs was also significantly increased (Figure 3C; median sizes: 389 420 μm^2 for AII_2 and 388 953 μm^2 for AII_1 compared with 225 078 μm^2 for C2). This size increase was not seen for iPSCs carrying the *RUNX1* deletion (Figure 3D), showing that RUNX1 haploinsufficiency did not affect the proliferation rate of GM lineage. Accordingly, the generation of mature monocytes and/or macrophages ($CD14^{high}CD15^{low}$) and granulocytes ($CD15^{high}$) in liquid medium (Figure 3E-F) revealed an increase in the proportion of GM populations carrying the *R174Q* mutation but not the *RUNX1* deletion. A significant twofold increase in the monocyte and/or macrophage output and a slight increase in granulocyte generation were detected for both patient lines with the *R174Q* mutation, but not for the patient lines with a *RUNX1* monoallelic deletion (Figure 3G-H). In accordance with our previous results,[4] the expression of the *NR4A3* gene was decreased in $CD34^+CD43^+$ progenitors sorted at day 14 from the 2 *R174Q* mutated iPSC clones, although no significant difference was observed between control and *RUNX1* monoallelic deleted cells (Figure 3I). These results indicate that only the *R174Q RUNX1* mutation leads to deregulation of the granulomonocytic compartment, which correlates with the downregulation of *NR4A3*.

RUNX1 transgene targeting corrects hematopoietic defects independently of the type of mutation

To exclude a role of iPSC line heterogeneity in the above-reported observation, we reintroduced a WT copy of the hemagglutinin (HA)-tagged *RUNX1* gene into one iPSC line of each pedigree and used zinc-finger nucleases to place this gene under control of *CD43* gene promoter into the "safe harbor" locus AAVS1 (Figure 4A).[27] Clones with homozygous integration were selected, and the overexpression of *HA-RUNX1* transcripts in $CD34^+CD43^+$ progenitors was checked (Figure 4B). In R174Q mutant cells, overexpression of RUNX1 was further verified by western blotting

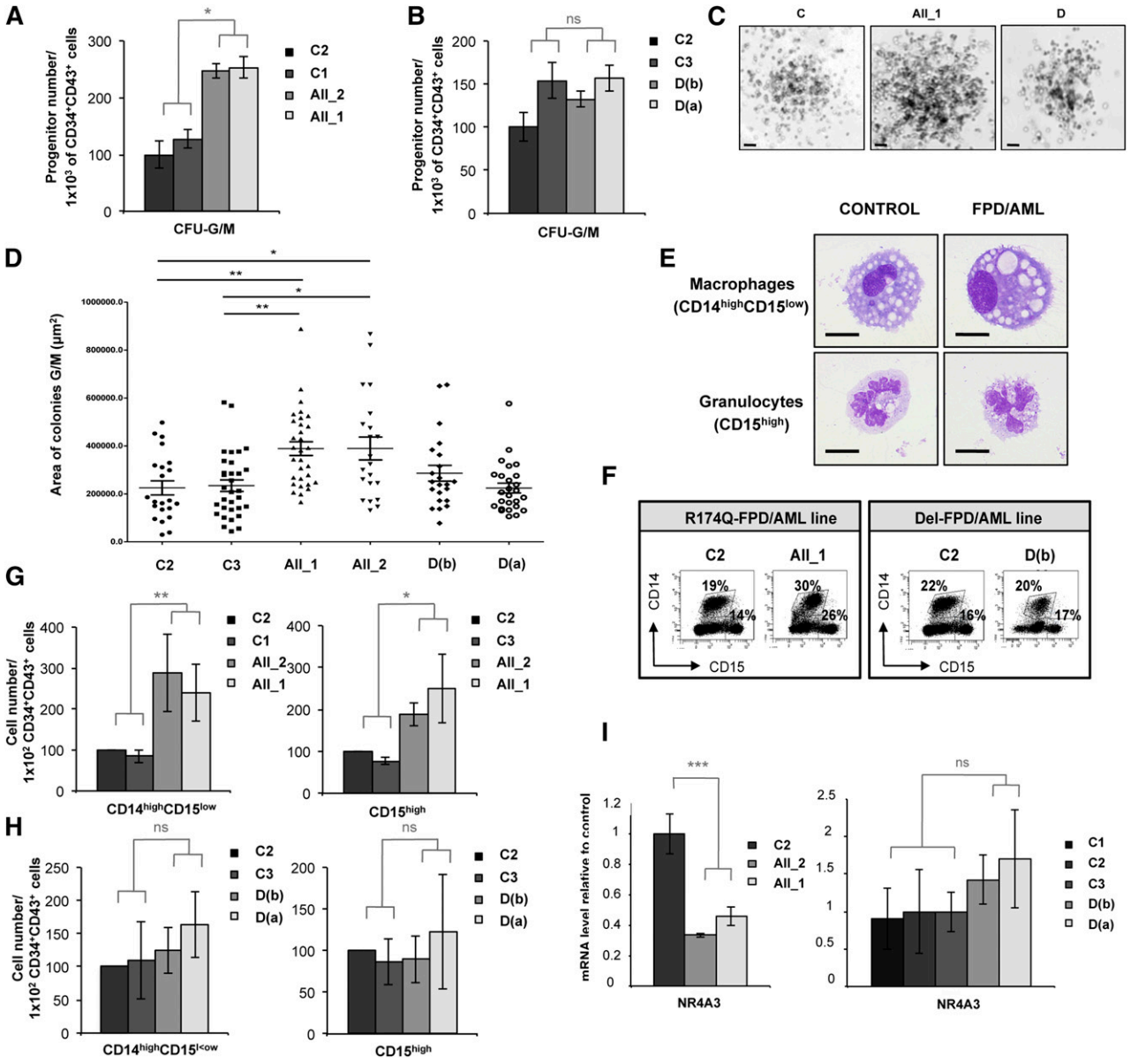

Figure 3. *RUNX1 R174Q* mutation but not *RUNX1* deletion affects the output of granulomonocytes. All_1, All_2 are iPSC clones of 2 patients from pedigree A; D(a) and D(b) are 2 clones of 1 patient from pedigree D; and C1, C2 and C3 are control iPS cell lines. Cell numbers were normalized in all experiments to those produced by the C2 clone. (A-D) $CD34^+CD43^+$ cells were sorted at day 14 and tested for their colony-forming potential in a methylcellulose assay. The histograms show (A) 1 representative experiment of 3 for pedigree A and (B) 1 representative experiment of 7 for pedigree D, each in triplicate. Error bars represent ± SD of triplicate. (C) Photos of granulomonocytic colonies (CFU-GM). Scale bar = 100 µm. (D) Area of more than 30 CFU-GM colonies obtained from each iPSC line was analyzed by AxioVisio 4.6 software. (E-H) Analysis of hematopoietic populations generated at day 21 from progenitors sorted at day 14. (E) May-Grünwald-Giemsa staining of monocytes and/or macrophages ($CD14^{high}CD15^{low}$) and granulocytes ($CD15^{high}$) derived from iPSCs. Scale bar = 10 µm. (F) FACS analysis of the GM cells in 1 representative experiment. (G-H) Absolute numbers of generated monocytes and/or macrophages ($CD14^{high}CD15^{low}$) and granulocytes ($CD15^{high}$) normalized to 1×10^2 plated progenitors. (G) The histograms show average of the cell number obtained in 5 independent experiments for monocytes and/or macrophages and in 3 for granulocytes for pedigree A. (H) The histograms show average of the cell number obtained in 4 independent experiments for pedigree D. Error bars represent ± SD of the average. (I) qRT-PCR analysis of *NR4A3* expression level in $CD34^+CD43^+$ cells in both A (left; n = 4) and D (right; n = 4) pedigrees. Data are normalized to *PPIA* transcript, and expression is compared with control C3. Error bars represent ± SD of triplicate. $^*P < .05$; $^{**}P < .01$; $^{***}P < .001$; Student *t* test. ns, nonsignificant.

(Figure 4C) and by measuring the expression of 2 direct RUNX1 targets, $p19^{INK4d}$ and MPL (Figure 4D). Reintroduction of WT RUNX1 induced a threefold increase in the number of MK progenitors for the deletion and a twofold increase for the R174Q mutant in comparison with the parent iPSC lines (Figure 4E). The gene correction also increased the number of erythroid progenitors produced by the FPD/AML iPSC lines by twofold for the deletion and by more than fivefold for the R174Q mutation compared with the parent iPSC lines (Figure 4F). Interestingly, the number of GM progenitors decreased to control levels in the transgene-targeted *R174Q* iPSC line, demonstrating reversal of the phenotype (Figure 4G).

Downregulation of RUNX1 in the H9 ESC line reproduced the dominant-negative phenotype

To determine whether the R174Q mutant has acquired a new function or leads to a loss of function, we transduced undifferentiated H9 ESCs with RUNX1 short hairpin RNA (shRNA) or control shRNA constructs. The use of shRUNX1_1 almost completely abolished the expression

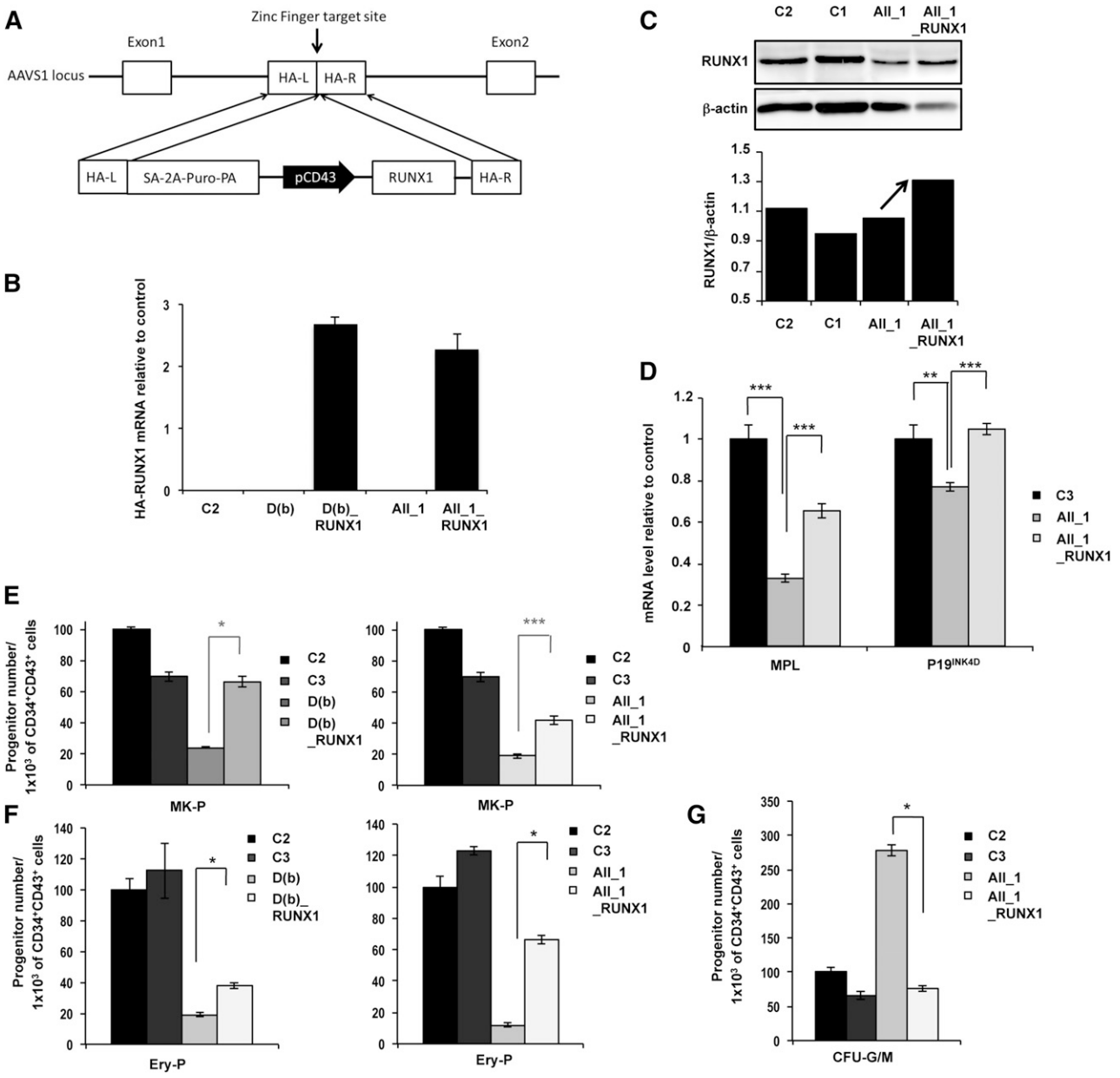

Figure 4. Genetic rescue by RUNX1 WT overexpression in FPD/AML iPSC lines. All_1 represents iPSC clones of 1 patient from pedigree A; D(b) represents 1 clone of 1 patient from pedigree D; All_1_RUNX1 and D(b)_RUNX1 are the iPSC clones overexpressing WT RUNX1; and C1, C2, and C3 are control iPSCs. (A) Gene correction strategy. The constitutively active *AAVS1* "safe harbor" locus is shown on the top line and the targeting construct is shown below. Complementary DNA (cDNA) expression cassette driving expression of WT *RUNX1* cDNA under the leukosialin promoter (pCD43) was inserted by zinc finger-mediated homologous recombination into intron 1 of *AAVS1*. HA: homologous arms left (L) and right (R); SA-2A-Puro-PA: puromycin drug resistance cassette. (B) Overexpression of HA-RUNX1 measured by qRT-PCR using forward primer in HA epitope and reverse primer in *RUNX1* cDNA. Error bars represent 95% confidence intervals (CIs). (C) Western blot analysis of total (endogenous and overexpressed) RUNX1. (D) qRT-PCR analysis of *MPL* and *P19*^{INK4D} expression level in MKs ($CD41^+CD42^+$) sorted at day 14. Data are normalized to *PPIA* transcript level, and expression is compared with control C3 (n = 3). (E-G) Cell numbers were normalized in all experiments to those produced by the C2 clone. (E-F) $CD34^+CD43^+$ cells were sorted at day 11 and tested for their colony-forming potential. (E) Assessment of MK progenitors in fibrin clot cultures (n = 3) (F) Assessment of erythroid progenitors in methylcellulose culture (n = 3) (G) $CD34^+CD43^+$ cells of pedigree A were sorted at day 14 and tested for their CFU-GM colony-forming potential in methylcellulose assay (n = 3). (D-G) Error bars represent ± SD of triplicate. *$P < .05$; **$P < .01$; ***$P < .001$; Student *t* test.

of RUNX1 at the protein level in the mesodermal cell population (Figure 5A). First we confirmed the central role of RUNX1 in hematopoiesis induction by showing a decrease in the generation of hematopoietic clones after RUNX1 knockdown[28] (supplemental Figure 5). Then, we assessed the colony-forming potential of $CD34^+CD43^+$ cells sorted at day 11, which demonstrated a more than 10-fold decrease in the number of erythrocyte progenitors (Figure 5B) and a threefold decrease in MK progenitors after RUNX1 knockdown (Figure 5C). In liquid medium, RUNX1 downregulation led to a decreased production of GPA^+ erythroid cells and $CD41^+CD42^+$ MKs at day 18 (Figure 5D-E). Next, we performed the same experiments with $CD34^+CD43^+$ cells sorted at day 14 and observed an increased number of CFU-GM colonies after RUNX1 knockdown (Figure 5F) and an increased number of $CD14^{high}CD15^{low}$ mature monocytes and/or macrophages and $CD15^{high}$ granulocyte populations at day 21 in liquid medium (Figure 5G). These results were validated by using a second shRNA, shRUNX1_2 (supplemental Figure 6). To further confirm that a decrease in RUNX1 activity is

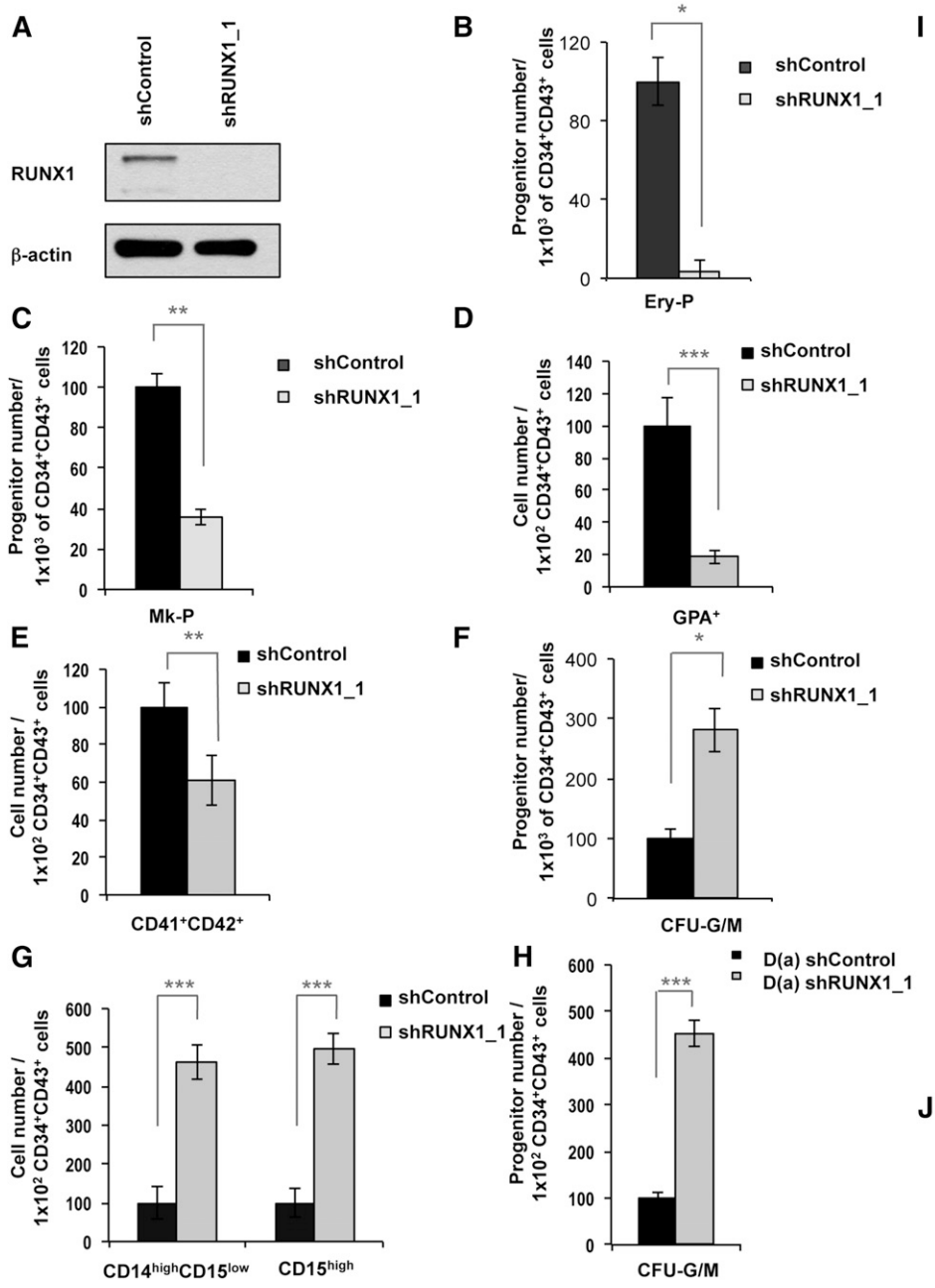

I

Gene	FC (+/- 1.5)	Lineage
HBM	-6,4284	E
GYPB	-6,334	E
GYPA	-4,9515	E
GYPE	-4,205	E
HBE1	-3,633	E
XK	-3,583	E
SPTA1	-3,472	E
HBA2	-3,272	E
ANK1	-3,246	E
EPB42	-2,852	E
HBB	-2,672	E
KLF1	-2,615	E
HBA1	-2,538	E
KEL	-2,354	E
HBQ1	-2,31	E
TRIM10	-2,266	E
TFRC	-1,881	E
RHCE	-1,79	E
SPTB	-1,679	E
EPOR	-1,602	E
GATA1	-1,93	E/MK
GATA2	-1,525	E/MK
CD226	-2,215	MK
ITGB3	-2,113	MK
TUBB1	-1,954	MK
VWA5A	-1,817	MK
PTGS1	-1,695	MK
ITGA2B	-1,692	MK
TBXAS1	-1,583	MK
ANO6	-1,576	MK
CX3CR1	-2,566	IM, IN
C4B	-1,849	IM, IN
CXCL3	-1,693	IM, IN
TREML2	-1,682	IM, IN
AIF1L	-1,549	IM, IN
IL18RAP	1,813	IM, IN
CLEC5A	1,835	IM, IN
IFI44	1,878	IM, IN
CST7	2,506	IM, IN
MB21D1	2,551	IM, IN
MPO	1,512	G/M
SCARA3	1,528	G/M
IRAK3	1,561	G/M
ELANE	1,676	G/M
SERPINB1	1,772	G/M
CTSG	3,558	G/M

J

Gene	FC
CDKN1A	-1.17
BBC3	-1.28
BTG2	-2.64
GADD45A	-1.32

Figure 5. RUNX1 knockdown in H9 ESC line and in an FPD/AML iPSC line with monoallelic *RUNX1* deletion leads to the same phenotype as the FPD/AML-DN iPSC line. (A-G) RUNX1 knockdown in H9 ESC line. (A) Analysis of RUNX1 protein expression in mesodermal population from control and shRUNX1_1 ESC lines. (B-C) $CD34^+$ $CD43^+$ cells were sorted at day 11 and tested for their colony-forming potential in methylcellulose assay and fibrin clot culture. (B) Assessment of erythroid progenitors in methylcellulose culture. (C) Assessment of MK progenitors in fibrin clot cultures. (B-C) The histograms show 1 representative experiment of 4 for erythroid progenitors and of 3 for MK progenitors, each in triplicate. Error bars represent ± SD of triplicate. (D-E) Analysis of hematopoietic populations generated at day 18 from progenitors sorted at day 11. (D) Absolute number of generated erythroid cells (GPA^+) normalized to 1×10^2 plated progenitors (n = 4). (E) Absolute number of generated MK cells ($CD41^+CD42^+$) normalized to 1×10^2 plated progenitors (n = 4). (D-E) The histograms show the average of 4 independent experiments. Error bars represent ± SD of average. (F) $CD34^+$ $CD43^+$ cells were sorted at day 14 and were tested for their CFU-GM colony-forming potential in methylcellulose assay. The histograms show 1 representative experiment of 4, each in triplicate. Error bars represent ± SD of triplicate. (G) Analysis of hematopoietic populations generated at day 21 from progenitors sorted at day 14. Absolute numbers of generated monocytes and/or macrophages ($CD14^{high}CD15^{low}$; n = 4) and granulocytes ($CD15^{high}$; n = 4) normalized to 1×10^2 plated progenitors. The histograms show the average of 4 experiments. Error bars represent ± SD of average. (H) RUNX1 knockdown in D(a) iPSC line with shRUNX1_1. $CD34^+CD43^+$ cells were sorted at day 14 and tested for their CFU-GM colony-forming potential in methylcellulose assay. The histograms show 1 representative experiment of 3, each in triplicate. Error bars represent ± SD of triplicate. (I-J) Transcriptome analysis of $CD34^+CD43^+$ progenitors derived from shControl and shRUNX1_1 transduced hESC line sorted at day 14 of culture. FC: fold change between cells transduced with shRUNX1_1 and shControl lentiviruses. Only genes with expression variation ± 1.5 and $P < .001$ (analysis of variance [ANOVA] test) are listed. (J) Variation in expression of genes involved in p53-dependent DNA damage response; $P < .001$ (ANOVA test). E, erythroid; G/M, granulomonocyte; I, immunity; IN, inflammation; MK, megakaryocyte. *$P < .05$; **$P < .01$; ***$P < .001$, Student *t* test.

crucial for the amplification of GM progenitors, we transduced the iPSC clone D(b) carrying a monoallelic *RUNX1* deletion with the shRUNX1_1. The additional decrease in RUNX1 level led to an increased number of CFU-GM colonies (Figure 5H).

Altogether, these results suggest that the differences between *R174Q* mutation and a monoallelic *RUNX1* deletion can be explained by RUNX1 dosage. An almost complete functional inhibition or deletion, but not a haploinsufficiency, leads to the deregulation of the GM compartment, which may contribute to leukemic development. Gene expression was then explored on hematopoietic $CD34^+CD43^+$ progenitors derived from shRUNX1_1 and shControl transduced hESCs and sorted at day14 of culture. On the 44 000 tested probe sets, 412 probe sets were deregulated at least 1.5-fold in shRUNX1_1 hESCs, with 327 probe sets decreased and 85 probe sets increased. A focus on hematopoietic genes (Figure 5I) identified 22 erythroid and 11 MK genes deregulated. In the GM compartment, we highlighted a global increase of the GM signature with an increase of 11 genes. These results confirmed that RUNX1 plays an important role in the commitment between erythrocyte/MK and GM lineages.

R174Q RUNX1 mutation but not haploinsufficiency leads to an increase in genomic instability

Gene expression analysis also demonstrated a slight decrease in 4 p53-dependent genes involved in DNA-damage response (Figure 5J). To explore the role of RUNX1 in genomic instability, we first sorted the $CD43^+$ hematopoietic cells at day 10 of culture from 2 FPD/AML iPSC lines with *R174Q* mutation and control iPSC lines. The accumulation of DNA double-strain breaks was investigated by using an antibody recognizing the phospho-histone H2AX (P-H2AX). As shown in Figure 6A-B, an increase in the number of P-H2AX–positive cells was observed in $CD43^+$ cells harboring the *R174Q* mutation compared with control cells, (from 50% for controls to about 70% for FPD/AML cells) as well as in the number of foci per cell. Because replication can induce P-H2AX foci formation, more particularly in highly proliferative erythroid cells that represent the majority of $CD43^+$ cells, we used P53BP1 as a marker of double-strain breaks. The number of cells presenting P53BP1 foci in $CD34^+CD43^+$ progenitors was increased in the population of R174Q mutant cells (from 50% in control C3 and C2 cells to 80% in R174Q mutant cells) (Figure 6C-D), whereas no increase was detected for cells with *RUNX1* deletion (Figure 6D). Then we evaluated the p53-dependent DNA-damage response pathway. In the entire $CD34^+CD43^+$ cell population, we did not detect any decrease in *p21*, *NOXA*, and *BAX* expression, whatever the *RUNX1* alteration (Figure 6E). Because the R174Q mutant cell line is characterized by an expansion of the GM lineage, we focused on this population. As shown in Figure 6F-G, an increase in the number of $CD14^+CD15^+$ cells positive for P53BP1 foci (from 26% for control cells to 53%) and in the number of foci per cell was detected for R174Q mutant cells. These results were confirmed by qRT-PCR, showing a strong decrease of *p21* and *GADD45A* and, to a lesser extent, *NOXA* and *BAX* gene expression in the $CD14^+CD15^+$ cell population (Figure 6H). Importantly, the number of cells showing P53BP1 foci was decreased to control levels. and the expression of all 4 genes was restored in FPD/AML iPSCs transduced with WT *RUNX1* (Figure 6G-H). Altogether, our results demonstrate that *R174Q RUNX1* mutation could predispose to leukemic transformation at least partly through NR4A3 downregulation and increased genomic instability in the GM compartment, which is not observed with cells harboring a *RUNX1* haploinsufficiency. Moreover, the additional decrease of RUNX1 activity in haploinsufficient iPS cells by the shRUNX1_1 led not only to an increase in CFU-GM progenitor number but also to a decrease in *p21* and *GADD45A* expression in the $CD14^+CD15^+$ cell population (supplemental Figure 7), attesting to the importance of the RUNX1 level in this phenotype.

Discussion

The current approaches used to explore FPD/AML pathogenesis remain limited, and access to patient primary cells is difficult because of the rarity of the disease. In addition, mouse models of *Runx1* alterations do not completely reflect the phenotype observed in FPD/AML patients (eg, adult mice with a conditional *Runx1* KO develop myeloproliferative syndrome/MDS rather than acute leukemia.[15] Thus, to further explore the mechanisms of dysmegakaryopoiesis and sensitivity to leukemic transformation related to diverse *RUNX1* alterations, we generated iPSC lines from 2 previously studied pedigrees: 1 with a DN-like mutation *R174Q* and 1 with a *RUNX1* monoallelic deletion. The 2 pedigrees are both associated with thrombocytopenia, whereas only the first pedigree is associated with AML.

The generation of hematopoietic progenitors during embryonic life occurs initially in large blood vessels by the formation of clusters derived from endothelial cells, a process that strikingly relies on the presence of RUNX1.[28,29] The number of human hematopoietic progenitors generated from FPD/AML iPSCs depends on the type of *RUNX1* alteration.[30] Here, we show that the knockdown of RUNX1 in ESCs limits the commitment to hematopoietic lineage at the clonal level.

The hematopoietic potential of different ESC[31] and iPSC lines can be very heterogeneous[32]; therefore, the analysis of hematopoietic lineages obtained from iPSCs was normalized to the number of initial hematopoietic progenitors and not of iPSCs. To isolate myeloid hematopoietic progenitors, the CD34 marker was used in combination with CD43 (leukosialin), which is an early and specific hematopoietic marker appearing before CD45 during development.[33]

In accordance with previously reported data,[34] we detected 2 discrete waves of primitive hematopoiesis with an increased capacity of the first $CD34^+CD43^+$ cells to generate primitive erythroid and MK progenitors compared with the $CD34^+CD43^+$ cells occurring later that demonstrate a granulomonocytic potential. By analyzing the clonogenic potential of hematopoietic $CD34^+CD43^+$ progenitors derived from FPD/AML iPSC clones, we observed a profound defect in the first wave giving rise to primitive erythroid and MK cells as well as in proplatelet formation from mature MKs, which is consistent with the dysmegakaryopoiesis observed in FPD/AML patients.[25] In addition, the same deregulation of myosin expression was found in MKs derived from both iPSC and adult $CD34^+$ cells,[25] confirming the validity of the iPSC model. These defects were independent of the type of *RUNX1* alteration (DN-like mutant or haploinsufficiency) and were partially restored after RUNX1 overexpression driven by the CD43 promoter in FPD/AML iPSC lines. Consistent with our results, defects in MK differentiation from iPSC lines derived from FPD/AML patients with *Y260X*,[35] *G172E*, *G143W*, and *N233fsX283*[30] *RUNX1* mutations were also reported.

Regarding the second wave, DN-like *R174Q RUNX1* mutation increased the proliferation rate and clonogenic potential of GM progenitors, which correlated with a decrease in *NR4A3* expression. Because a similar phenotype was also observed after almost complete RUNX1 knockdown in hESCs, we can conclude that R174Q mutant is close to a complete loss of function. Conversely, the half decrease in RUNX1 dosage resulting from *RUNX1* deletion did not

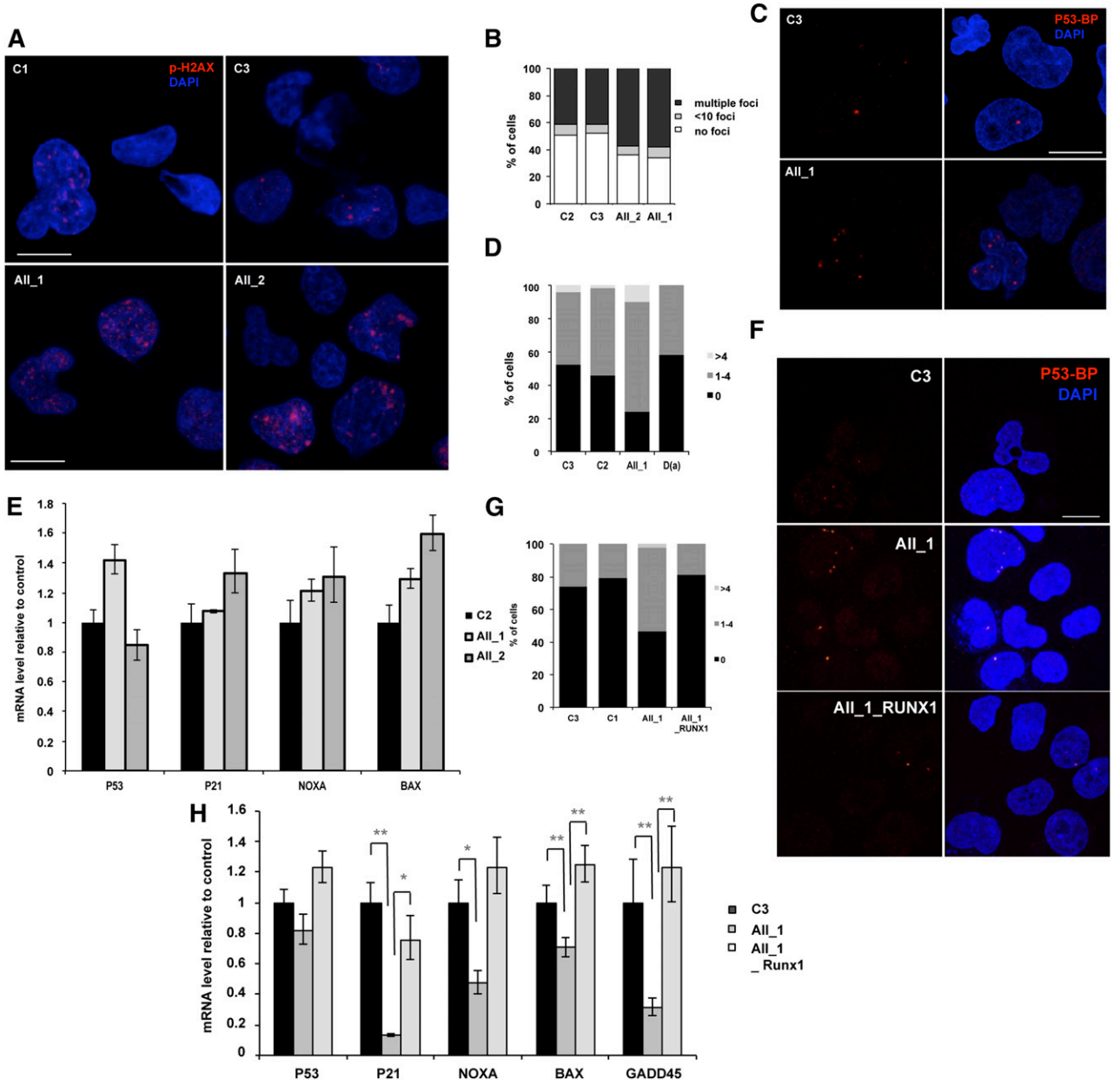

Figure 6. RUNX1 DN-like mutant induces increased genomic instability compared with RUNX1 haploinsufficiency. All_1 and All_2 are iPSC clones of 2 patients from pedigree A; D(a) is 1 clone of 1 patient from pedigree D; All_1_RUNX1 is the iPSC clone All_1 overexpressing WT RUNX1; D(a)_shRUNX1_1 is the iPSC clone D(a) after RUNX1 knockdown by shRUNX1_1; and C2 and C3 are control iPSC lines. (A-B) $CD43^+$ cells and (C-E) $CD34^+CD43^+$ cells were sorted at day 14 of culture. (A,C) Representative photos are shown; nucleus is stained with 4,6 diamidino-2-phenylindole (DAPI; blue) and double-strain breaks (DSBs) are stained (A) with P-H2AX (red) or (C) with p53-BP1 (red). The number of (B) P-H2AX and (D) P53-BP1 foci per 50 counted cells is shown. One representative experiment of 4 is shown ($P < .0001$ for the increase in P-H2AX–positive cells; $P = .0164$ for the increase in P53BP1-positive cells in pedigree A). (E) qRT-PCR analysis of different p53-dependent genes in $CD34^+CD43^+$ cells. Data are normalized to *PPIA* transcript level and expression is compared with control C2. The histograms show 1 representative experiment of 3, each in triplicate. Error bars represent 95% CIs. (F-H) $CD14^+CD15^+$ cells were sorted at day 15 of culture. (F) Representative photos are shown; nucleus is stained with DAPI (blue) and DSBs are stained with P53BP1 (red). (G) The number of P53BP1 foci per 100 counted cells is shown. One representative experiment of 3 is shown ($P = .0017$ for the increase in P53BP1-positive cells in All_1). (H) qRT-PCR analysis of different p53-dependent genes in $CD14^+CD15^+$ cells. Data are normalized to *PPIA* transcript level and expression is compared with control C3. The histograms show 1 representative experiment of 3, each in triplicate. Error bars represent 95% CIs. $^*P < .05$; $^{**}P < .01$; $^{***}P < .001$; Student *t* test.

affect the GM lineages and *NR4A3* expression and further attest that DN-like R174Q mutant could contribute to the induction of a preleukemic state by increasing the GM progenitor compartment, the main cell target for AML. Even if our differentiation protocol allows us to study only primitive hematopoiesis, these results are in agreement with observations made in adult progenitors from FPD/AML patients harboring the *R174Q* mutation,[4] in which the increase in the GM compartment has been associated with NR4A3 downregulation by RUNX1. Furthermore, the importance of NR4A3 dosage was already highlighted in the induction of myeloproliferative neoplasms and AML in *NR4A3* KO mouse models.[36-38] Contrary to our results showing the amplification of GM lineage after almost complete knockdown of *RUNX1* or with DN-like *R174Q* mutation, this amplification was not observed with *N233fsX283* mutation,[30] which is highly associated with AML. However, this last mutation induces a deep defect in the generation of hematopoietic progenitors, which could in some way also be a preleukemic state similar to that in some aplastic anemias.

To the best of our knowledge, this is the first study that clarifies the differences in granulomonocytic lineage between a haploinsufficiency alone and the DN-like R174Q RUNX1 mutant. These differences are clearly dependent on the protein dosage. The R174Q mutant behaving as a DN may preclude the formation of active core-binding complexes. This hypothesis becomes even more plausible when we take the following into account: (1) the report that certain RUNX1 mutants, including R174Q, bind CBFβ more strongly than the WT,[3] and mouse models of CBFβ deficiency recapitulate the phenotype observed with this RUNX1 mutant[39]; (2) the results obtained with the 2 shRUNX1 in hESCs in which abrogation of RUNX1 leads to a phenotype close to R174Q; and (3) the rescue of DN phenotype by overexpression of WT RUNX1 probably by changing the equilibrium of WT vs mutant binding to CBFβ. A recent study highlighted the complexity of RUNX1 dosage by reporting that a minimal dosage is necessary for MLL fusion leukemia.[40] Here, we show that a very low level of RUNX1 increases the proliferative rate and genomic instability of GM progenitors that could be at the origin of the preleukemic state in patients, whereas a half-decrease in RUNX1 level leads to thrombocytopenia alone. However, it should be noted that leukemia development was described in 1 pedigree with hemizygous *RUNX1* deletion,[1] attesting that the simple dichotomy of DN vs haploinsufficient mutant for AML development is not so clear and that other genetic events could also contribute to the development of leukemia. However, our results are consistent with the importance of the transcription factor level in malignant disorders. This is underscored by the example of PU.1, which needs to be decreased to less than 80% for inducing AML[41] whereas a haploinsufficiency has no effect.[42,43]

Finally, we demonstrate that a RUNX1 loss of function leads to an increase in genomic instability linked to a decreased expression of p53-dependent genes and to an increase in the number of P53BP1 foci. Moreover, in the presence of the R174Q mutant, 10-fold more mutations occurred during the reprogramming process as compared with monoallelic *RUNX1* deletion and control cell lines.[44] Consistent with these results, a novel role for RUNX1 during DNA-damage response has been recently identified. Indeed, it cooperates with p53 after DNA damage and is recruited onto p53 target gene promoters.[45] In addition, a decreased expression of the direct RUNX1 target *GADD45A*, encoding for a sensor of DNA stress, was observed in bone marrow cells from MDS/AML patients harboring a *RUNX1* mutation in the C-terminal domain.[19] GADD45A was shown to be activated synergistically by RUNX1 and p53. Interestingly, Michaud et al[46] previously reported a global genomic instability linked to RUNX1 impairment, and the incidence of *RUNX1* mutations in therapy-related MDS and AML is particularly high, revealing again a potential role of RUNX1 in genomic instability.[47]

In conclusion, whereas analysis of mouse models failed to identify any defect in primitive hematopoiesis, we show for the first time that *RUNX1* germline alterations affect human embryonic hematopoiesis, particularly the generation of primitive erythroid and MK cells. As already described by others,[30,35] defects in the generation of mature MK cells do not depend on the type of *RUNX1* variants. Conversely, a DN R174Q mutant of RUNX1 increases the proliferative rate and induces a genomic instability of GM progenitors, thereby contributing to development of a preleukemic state.

Acknowledgments

The authors thank P. Rameau and Y. Lécluse for flow cytometry cell sorting and analysis (Integrated Research Cancer Institute in Villejuif, Gustave Roussy, Villejuif, France), Dr G. Meurice for the comparative genome hybridization analysis (Plateforme de Bioinformatique, Gustave Roussy, Villejuif, France), Dr P. Opolon for the teratomas analysis (Plateforme d' Histopathologie, Gustave Roussy, Villejuif, France), P. Nusbaum and A. Hubas for patient fibroblast culture (Banque de Cellules directed by Pr. J. Chelly, Hôpital Cochin, Paris, France), Pr. Jonveaux (Centre Hospitalier Universitaire de Nancy, Nancy, France) for his advice, Dr A. Foudi and Dr G. Mostoslavsky (Boston University and Boston Medical Center, Boston, MA) for providing lentiviral vector STEMCCA, Drs A. Galy and S. Charrier for providing lentiviral vector pRRLcpptPGKGFP-WPRE-Alb (Genethon, Evry, France), and the patients for participating in this study.

This work was supported by grants from the Agence Nationale de la Recherche (ANR-physiopathology, ANR-jeunes chercheurs) (H.R.), the Centre de Référence des Pathologies Plaquettaires, and the Association pour la Recherche sur le Cancer (projet libre, I.P. 2012 and W.V. 2009). The Comparative Genome Hybridization array was funded by the apprenticeship tax (TA2011). Labex Globule Rouge-Excellence (I.P., W.V.) was funded by the "Investissements d'avenir" program. I.A.-D. was supported by a doctoral fellowship from the Association pour la Recherche sur le Cancer. N.D. and W.V. are recipients of a research fellowship from Centre Hospitalier Universitaire Bordeaux (N.D.) and from the Institute Gustave Roussy-INSERM (W.V.).

Authorship

Contribution: I.A.-D., V.T.M., W.V., and H.R. designed experiments; I.A.-D., V.T.M., N.B., D.B., C.T., C.L., T.L., O.B., L.T., and J.A.M. performed experiments; I.A.-D., V.T.M., L.T., G.T., and H.R. analyzed data; B.L. and R.F. provided clinical and biological follow-up of patients; N.D., I.P., E.S., R.F., D.L.F., M.J.W., and W.V. discussed the techniques and results; H.R. supervised the work; and I.A.-D., V.T.M., W.V., and H.R. wrote the paper.

Conflict-of-interest disclosure: The authors declare no competing financial interests.

Correspondence: Hana Raslova, INSERM UMR1009, Institut Gustave Roussy, 114 rue Edouard Vaillant, 94805 Villejuif Cedex, France; e-mail: hraslova@igr.fr.

References

1. Song WJ, Sullivan MG, Legare RD, et al. Haploinsufficiency of CBFA2 causes familial thrombocytopenia with propensity to develop acute myelogenous leukaemia. *Nat Genet.* 1999;23(2):166-175.
2. Béri-Dexheimer M, Latger-Cannard V, Philippe C, et al. Clinical phenotype of germline RUNX1 haploinsufficiency: from point mutations to large genomic deletions. *Eur J Hum Genet.* 2008;16(8):1014-1018.
3. Michaud J, Wu F, Osato M, et al. In vitro analyses of known and novel RUNX1/AML1 mutations in dominant familial platelet disorder with predisposition to acute myelogenous leukemia: implications for mechanisms of pathogenesis. *Blood.* 2002;99(4):1364-1372.
4. Bluteau D, Gilles L, Hilpert M, et al. Down-regulation of the RUNX1-target gene NR4A3 contributes to hematopoiesis deregulation in familial platelet disorder/acute myelogenous leukemia. *Blood.* 2011;118(24):6310-6320.

5. Preudhomme C, Renneville A, Bourdon V, et al. High frequency of RUNX1 biallelic alteration in acute myeloid leukemia secondary to familial platelet disorder. *Blood.* 2009;113(22):5583-5587.
6. Grimwade D, Hills RK, Moorman AV, et al; National Cancer Research Institute Adult Leukaemia Working Group. Refinement of cytogenetic classification in acute myeloid leukemia: determination of prognostic significance of rare recurring chromosomal abnormalities among 5876 younger adult patients treated in the United Kingdom Medical Research Council trials. *Blood.* 2010;116(3):354-365.
7. Gaidzik VI, Bullinger L, Schlenk RF, et al. RUNX1 mutations in acute myeloid leukemia: results from a comprehensive genetic and clinical analysis from the AML study group. *J Clin Oncol.* 2011; 29(10):1364-1372.
8. Tang JL, Hou HA, Chen CY, et al. AML1/RUNX1 mutations in 470 adult patients with de novo acute myeloid leukemia: prognostic implication and interaction with other gene alterations. *Blood.* 2009;114(26):5352-5361.
9. Schnittger S, Dicker F, Kern W, et al. RUNX1 mutations are frequent in de novo AML with noncomplex karyotype and confer an unfavorable prognosis. *Blood.* 2011;117(8):2348-2357.
10. Itzykson R, Kosmider O, Renneville A, et al. Prognostic score including gene mutations in chronic myelomonocytic leukemia. *J Clin Oncol.* 2013;31(19):2428-2436.
11. Kohlmann A, Grossmann V, Klein HU, et al. Next-generation sequencing technology reveals a characteristic pattern of molecular mutations in 72.8% of chronic myelomonocytic leukemia by detecting frequent alterations in TET2, CBL, RAS, and RUNX1. *J Clin Oncol.* 2010;28(24): 3858-3865.
12. Bejar R, Stevenson K, Abdel-Wahab O, et al. Clinical effect of point mutations in myelodysplastic syndromes. *N Engl J Med.* 2011;364(26):2496-2506.
13. Flach J, Dicker F, Schnittger S, et al. An accumulation of cytogenetic and molecular genetic events characterizes the progression from MDS to secondary AML: an analysis of 38 paired samples analyzed by cytogenetics, molecular mutation analysis and SNP microarray profiling. *Leukemia.* 2011;25(4):713-718.
14. Okuda T, van Deursen J, Hiebert SW, Grosveld G, Downing JR. AML1, the target of multiple chromosomal translocations in human leukemia, is essential for normal fetal liver hematopoiesis. *Cell.* 1996;84(2):321-330.
15. Growney JD, Shigematsu H, Li Z, et al. Loss of Runx1 perturbs adult hematopoiesis and is associated with a myeloproliferative phenotype. *Blood.* 2005;106(2):494-504.
16. Ichikawa M, Asai T, Saito T, et al. AML-1 is required for megakaryocytic maturation and lymphocytic differentiation, but not for maintenance of hematopoietic stem cells in adult hematopoiesis. *Nat Med.* 2004;10(3):299-304.
17. Yokomizo T, Hasegawa K, Ishitobi H, et al. Runx1 is involved in primitive erythropoiesis in the mouse. *Blood.* 2008;111(8):4075-4080.
18. Takahashi K, Yamanaka S. Induction of pluripotent stem cells from mouse embryonic and adult fibroblast cultures by defined factors. *Cell.* 2006;126(4):663-676.
19. Satoh Y, Matsumura I, Tanaka H, et al. C-terminal mutation of RUNX1 attenuates the DNA-damage repair response in hematopoietic stem cells. *Leukemia.* 2012;26(2):303-311.
20. Klimchenko O, Mori M, Distefano A, et al. A common bipotent progenitor generates the erythroid and megakaryocyte lineages in embryonic stem cell-derived primitive hematopoiesis. *Blood.* 2009;114(8):1506-1517.
21. Amit M, Carpenter MK, Inokuma MS, et al. Clonally derived human embryonic stem cell lines maintain pluripotency and proliferative potential for prolonged periods of culture. *Dev Biol.* 2000; 227(2):271-278.
22. Mills JA, Wang K, Paluru P, et al. Clonal genetic and hematopoietic heterogeneity among human-induced pluripotent stem cell lines. *Blood.* 2013; 122(12):2047-2051.
23. Kim K, Doi A, Wen B, et al. Epigenetic memory in induced pluripotent stem cells. *Nature.* 2010; 467(7313):285-290.
24. Polo JM, Liu S, Figueroa ME, et al. Cell type of origin influences the molecular and functional properties of mouse induced pluripotent stem cells. *Nat Biotechnol.* 2010;28(8):848-855.
25. Bluteau D, Glembotsky AC, Raimbault A, et al. Dysmegakaryopoiesis of FPD/AML pedigrees with constitutional RUNX1 mutations is linked to myosin II deregulated expression. *Blood.* 2012; 120(13):2708-2718.
26. Lordier L, Bluteau D, Jalil A, et al. RUNX1-induced silencing of non-muscle myosin heavy chain IIB contributes to megakaryocyte polyploidization. *Nat Commun.* 2012;3:717.
27. Tiyaboonchai A, Mac H, Shamsedeen R, et al. Utilization of the AAVS1 safe harbor locus for hematopoietic specific transgene expression and gene knockdown in human ES cells. *Stem Cell Res (Amst).* 2014;12(3):630-637.
28. Chen MJ, Yokomizo T, Zeigler BM, Dzierzak E, Speck NA. Runx1 is required for the endothelial to haematopoietic cell transition but not thereafter. *Nature.* 2009;457(7231):887-891.
29. Liakhovitskaia A, Gribi R, Stamateris E, et al. Restoration of Runx1 expression in the Tie2 cell compartment rescues definitive hematopoietic stem cells and extends life of Runx1 knockout animals until birth. *Stem Cells.* 2009;27(7): 1616-1624.
30. Sakurai M, Kunimoto H, Watanabe N, et al. Impaired hematopoietic differentiation of RUNX1-mutated induced pluripotent stem cells derived from FPD/AML patients. *Leukemia.* 2014;28(12): 2344-2354.
31. Chang KH, Nelson AM, Fields PA, et al. Diverse hematopoietic potentials of five human embryonic stem cell lines. *Exp Cell Res.* 2008;314(16): 2930-2940.
32. Maclean GA, Menne TF, Guo G, et al. Altered hematopoiesis in trisomy 21 as revealed through in vitro differentiation of isogenic human pluripotent cells. *Proc Natl Acad Sci USA.* 2012; 109(43):17567-17572.
33. Vodyanik MA, Thomson JA, Slukvin II. Leukosialin (CD43) defines hematopoietic progenitors in human embryonic stem cell differentiation cultures. *Blood.* 2006;108(6): 2095-2105.
34. Rafii S, Kloss CC, Butler JM, et al. Human ESC-derived hemogenic endothelial cells undergo distinct waves of endothelial to hematopoietic transition. *Blood.* 2013;121(5):770-780.
35. Connelly JP, Kwon EM, Gao Y, et al. Targeted correction of RUNX1 mutation in FPD patient-specific induced pluripotent stem cells rescues megakaryopoietic defects [published online ahead of print August 11, 2014]. *Blood.* 2014.
36. Ramirez-Herrick AM, Mullican SE, Sheehan AM, Conneely OM. Reduced NR4A gene dosage leads to mixed myelodysplastic/myeloproliferative neoplasms in mice. *Blood.* 2011;117(9): 2681-2690.
37. Boudreaux SP, Ramirez-Herrick AM, Duren RP, Conneely OM. Genome-wide profiling reveals transcriptional repression of MYC as a core component of NR4A tumor suppression in acute myeloid leukemia. *Oncogenesis.* 2012;1:e19.
38. Mullican SE, Zhang S, Konopleva M, et al. Abrogation of nuclear receptors Nr4a3 and Nr4a1 leads to development of acute myeloid leukemia. *Nat Med.* 2007;13(6):730-735.
39. Satpathy AT, Briseño CG, Cai X, et al. Runx1 and Cbfβ regulate the development of Flt3+ dendritic cell progenitors and restrict myeloproliferative disorder. *Blood.* 2014;123(19):2968-2977.
40. Goyama S, Schibler J, Cunningham L, et al. Transcription factor RUNX1 promotes survival of acute myeloid leukemia cells. *J Clin Invest.* 2013; 123(9):3876-3888.
41. Rosenbauer F, Wagner K, Kutok JL, et al. Acute myeloid leukemia induced by graded reduction of a lineage-specific transcription factor, PU.1. *Nat Genet.* 2004;36(6):624-630.
42. Scott EW, Fisher RC, Olson MC, Kehrli EW, Simon MC, Singh H. PU.1 functions in a cell-autonomous manner to control the differentiation of multipotential lymphoid-myeloid progenitors. *Immunity.* 1997;6(4):437-447.
43. Olson MC, Scott EW, Hack AA, et al. PU. 1 is not essential for early myeloid gene expression but is required for terminal myeloid differentiation. *Immunity.* 1995;3(6):703-714.
44. Gore A, Li Z, Fung HL, et al. Somatic coding mutations in human induced pluripotent stem cells. *Nature.* 2011;471(7336):63-67.
45. Wu D, Ozaki T, Yoshihara Y, Kubo N, Nakagawara A. Runt-related transcription factor 1 (RUNX1) stimulates tumor suppressor p53 protein in response to DNA damage through complex formation and acetylation. *J Biol Chem.* 2013;288(2):1353-1364.
46. Michaud J, Simpson KM, Escher R, et al. Integrative analysis of RUNX1 downstream pathways and target genes. *BMC Genomics.* 2008;9:363.
47. Harada H, Harada Y, Tanaka H, Kimura A, Inaba T. Implications of somatic mutations in the AML1 gene in radiation-associated and therapy-related myelodysplastic syndrome/acute myeloid leukemia. *Blood.* 2003;101(2):673-680.

2015 125: 930-940
doi:10.1182/blood-2014-06-585513 originally published online December 9, 2014

Level of RUNX1 activity is critical for leukemic predisposition but not for thrombocytopenia

Iléana Antony-Debré, Vladimir T. Manchev, Nathalie Balayn, Dominique Bluteau, Cécile Tomowiak, Céline Legrand, Thierry Langlois, Olivia Bawa, Lucie Tosca, Gérard Tachdjian, Bruno Leheup, Najet Debili, Isabelle Plo, Jason A. Mills, Deborah L. French, Mitchell J. Weiss, Eric Solary, Remi Favier, William Vainchenker and Hana Raslova

Blood (print ISSN 0006-4971, online ISSN 1528-0020), is published weekly by the American Society of Hematology, 2021 L St, NW, Suite 900, Washington DC 20036.